Vol. 62: 99–113, 2015
doi: 10.3354/cr01266

CLIMATE RESEARCH
Clim Res

Published online January 14

Characteristics of drought in the arid region of northwestern China

Huaijun Wang[1, 2], Yaning Chen[1,*], Yingping Pan[1, 2]

[1]State Key Laboratory of Desert and Oasis Ecology, Xinjiang Institute of Ecology and Geography, Chinese Academy of Sciences (CAS), Urumqi, Xinjiang 830011, China
[2]University of Chinese Academy of Sciences, Beijing 100049, China

ABSTRACT: Drought evolution from 1960 to 2010 and its teleconnections were analyzed by utilizing the monthly Standardized Precipitation Evapotranspiration Index (SPEI) in the arid region of northwestern China. To assess the temporal pattern of drought as multi-scalar events, the SPEI was calculated for short-term (1 and 3 mo), medium-term (6 and 12 mo), and long-term droughts (24 and 48 mo). The results showed (1) step changes occurred in 1986; droughts occurred frequently before 1986, and wet periods prevailed after 1986. Generally, the period of 1973–1983 showed the highest drought activity, while 1993–1998 showed the lowest. (2) Annual and seasonal SPEI demonstrated significant upward trends, especially for the stations around the Tarim River Basin, implying that the study area had become wetter. (3) Interannual periods and decadal periods were observed for the whole study area and sub-regions. Moreover, patterns of period characteristics became more apparent at longer time scales. (4) The Indian Ocean Basin-Wide mode (IOBW) and Pacific Decadal Oscillation (PDO) may be the dominant forces, with the largest correlation coefficients in the whole study area. For the Xinjiang region, the simultaneous Arctic Oscillation (AO) and North Atlantic Oscillation (NAO) play an important role in drought evolution, especially from January to March. Lag times between climate indices and SPEI may exist in this arid region, and current droughts may be affected by the preceding climate indices.

KEY WORDS: Drought · SPEI · Teleconnections · Arid region of China

1. INTRODUCTION

Drought is a recurring extreme climate event over land, characterized by below-normal precipitation over a period of several months to several years, or even a few decades (Dai 2011). Few extreme events are as economically and ecologically disruptive as drought, which affects millions of people in the world annually. In fact, severe drought conditions have serious impacts on agriculture, water resources, tourism, ecosystems, and basic human welfare (Santos et al. 2010). In the arid region of northwestern China, which is one of the driest areas of the world, agriculture represents the main activity sector, and the occurrence of drought dramatically affects agricultural output.

Droughts have dramatically increased in numbers and intensity in many parts of the world. It is estimated that in European Union (EU) counties, the number of affected people has increased by 20% over the last 3 decades (Vangelis et al. 2011). Since 1991, the yearly average economic impact of drought in Europe is €5.3 billion, with the economic damage of the 2003 drought in Europe accounting for at least €8.7 billion (European Communities 2007). During the last 2 decades, the impact of droughts in the United States has also increased significantly, with an increased number of droughts and an increase in their severity (Changnon et al. 2000). From 1980 to 2003 in the United States, drought alone accounted for 41.2% of the total cost of all weather-related disasters (Ross & Lott 2003). In Australia, drought is also

*Corresponding author: chenyn@ms.xjb.ac.cn

a common disaster, e.g. the 2006 drought reduced the national winter cereal crop by 36% (Wong et al. 2010). In Africa, drought-related disasters are particularly severe. Since the late 1960s, the Sahel semi-arid region in west Africa between the Sahara desert and the Guinea coast rainforest has experienced droughts of unprecedented severity in recorded history; it has had a truly devastating impact on this ecologically vulnerable region (Zeng 2003, Mortimore 2010). Due partly to increasing temperatures, increasing frequency of El Niño events and reductions in the number of days with precipitation, the production of rice, maize, and wheat in the past few decades has declined in many parts of Asia, especially from 1999 to 2000. In fact, up to 60 million people in central and southwest Asia were affected by a persistent multi-year drought (Mishra & Singh 2010).

Similarly, China has also suffered severe drought in the past few decades. Since the 1980s, the continued drought in northern China has caused enormous losses, creating even more shortages of already-strained water resources; blowing sand has also increased significantly (Li 2012). For example, Yunnan Province and its surrounding area have suffered a severe drought for more than 10 yr, especially since 2010 (Wang & Meng 2013). A serious drought was also observed in eastern northwest China from 1994 to 1995, which caused the summer grain to decrease by 32% (Zhang & Fang 1995). Droughts have occurred frequently since the 1990s in northwest China, and the average annual affected area in the 1990s reached 3.57×10^6 ha.

Drought indices are the foundation for monitoring, evaluating, and assessing drought occurrence. Scholars have proposed various drought indices (Jinsong et al. 2007); among them, the Palmer Drought Severity Index (PDSI) (Vicente-Serrano et al. 2011a) is one of the most widely utilized. Specifically, it is a climatic water balance that considers precipitation, evapotranspiration anomalies, and soil water-holding capacity. The PDSI has a fixed temporal scale, which does not permit different drought types (e.g. hydrological, meteorological, agricultural, and socioeconomic) to be distinguished. This is an important shortcoming in PDSI because drought is a multi-scale phenomenon. The Standardized Precipitation Index (SPI) is another widely used index, which can calculate varying time scales and monitor droughts with respect to different usable water resources (Lorenzo-Lacruz et al. 2010). However, the SPI has the important disadvantage in that it is based only on precipitation data; thus, it does not consider other critical variables, such as evapotranspiration, which can have a marked influence on drought conditions. For such reasons, Vicente-Serrano et al. (2010) formulated a new drought index, i.e. the Standard Precipitation Evapotranspiration Index (SPEI), based on precipitation and potential evapotranspiration (PET). The SPEI considers not only precipitation, but also evapotranspiration (PET) data in its calculation, allowing for a more complete approach to explore the effects of climate change on drought conditions. Some region studies, such as the NW Iberian Peninsula (Vicente-Serrano et al. 2011b), the Mediterranean Region (Vicente-Serrano et al. 2011c), Tagus River (Central Spain) (Lorenzo-Lacruz et al. 2010), China (Yu et al. 2014), and Tarim River of China (Tao et al. 2014) have indicated that the SPEI can describe drought evolution well, and is also more appropriate for comparing the drought severity of diverse climates.

Atmospheric teleconnections are defined as the distant regions affected by large scale changes in atmospheric circulation patterns. Many indices have been developed to measure the variability of oceanic and atmospheric parameters. These include the Southern Oscillation Index (SOI), the Multivariate ENSO Index (MEI), the Pacific North American (PNA) index, the Pacific Decadal Oscillation (PDO) index, the North Atlantic Oscillation (NAO) index, the Indian Ocean Basin-Wide mode (IOBW) and the Arctic Oscillation (AO) index (Mishra & Singh 2010). Many studies have been carried out to elucidate the relationship between these indices and drought. For example, Hoerling & Kumar (2003) found that the 1998–2002 prolonged and widespread drought in the United States, southern Europe, and southwest Asia was linked to a common oceanic influence. Barlow et al. (2002) pointed out that drought in central and southwest Asia is related to a combination of the prolonged duration of La Niña and unusually warm SSTs in the west Pacific. SST is another factor affecting the wet/dry conditions in northwest China: the region is humid in a typical ENSO warm state, and dry in a typical ENSO cold state (Su & Wang 2006). Some investigations have also demonstrated that the wet/dry climate in northwestern China has a significant positive correlation with PDO (Ma & Shao 2006). Yang & Shi (2002) showed that the spring anomalies in Xinjiang show a good correspondence to the Indian Ocean SSTA. The AO and NAO are important factors affecting the climate in the Northern Hemisphere, and also exert important effects on the climate of northwestern China.

Characterization of the temporal variability of droughts can be very useful for achieving adequate

water resource management. For this reason, this study aims to identify the temporal patterns of droughts within the arid region of northwestern China. In addition, the identification of cycles of dry and wet events in those temporal patterns was achieved based on wavelet transform analysis. Drought is generally driven by extremes in the natural variations of climate, which are forced by the internal interactions of the atmosphere and feedback from the oceans and land surfaces. Thus, this study also evaluates the roles played by well-known large modes of atmospheric circulation variability on the regional inter-annual variability of drought indices in the arid region of northwest China.

2. STUDY AREA, DATA, AND METHODS

2.1. Study area

The arid region of study is located in the northwestern part of China, ranging from 34° to 50° N and from 73° to 108° E, including the provinces of Xinjiang, Gansu, the western part of Inner Mongolia, and the northern part of Ningxia. China's northwestern arid endorheic drainage basins cover a considerable area of 2.53 million km^2, located to the west of the Helanshan Mountains in the Ningxia Hui Autonomous Region, and to the west of the Ushaoling Mountains in Gansu Province. Among these basins is the Tarim Basin, Tsaidam Basin, Badanjilin Desert, Tengger Desert, and others in the northern Xinjiang Uygur Autonomous Regions, the Alashangqi desert in western Inner Mongolia, and the Hexi Corridor Gobi-desert in Gansu Province (Liu et al. 2010). The climate of the arid region is typical of inner-continental land masses, with a wide temperature range, low precipitation, and low humidity. The climate is dominated by continental arid conditions, with lesser effects from the East Asian Monsoon. In order to clearly describe the spatial distribution of drought, the present study divides the arid region into 4 parts, i.e. north Xinjiang, the Tianshan mountain areas, south Xinjiang, and the Hexi Corridor (Fig. 1), based on their climate characteristics and topography.

2.2. Data

Monthly climate variables (including temperature, daily maximum temperature, daily minimum temperature, wind speed at 2 m height, relative humidity, and daily bright sunshine hours) covering the arid region of China were provided by National Climate Center (NCC) of the China Meteorological Administration (CMA). For this area, 84 stations passed the internal homogeneity check of the China National Meteorological Center (CNMC), including the moving *t*-test (Peterson et al. 1998), standard normal homogeneity test (Alexandersson 1986), and the departure accumulating method (Buishand 1982). Stations that were installed after 1960 and those with data gaps were excluded. As a result, 75 weather stations with records for 51 yr (January 1960 to February 2011) were selected.

In order to identify the physical mechanisms of circulation patterns, we selected several climate indices that may affect drought evolution in the study area. The AO and NAO data come from Jianping Li (www.cru.uea.ac.uk/data/), and the MEI data are provided by the UK Met Office (UKMO) Hadley Centre (www.metoffice.gov.uk/hadobs/hadsst2/). Monthly PDO and IOBW series for the main teleconnections were obtained from the JISAO website (http://jisao.washington.edu/data_sets/) and the NCC (http://cmdp.ncc.cma.gov.cn/cn/index.htm), respectively.

2.3. Methods

The method of computing the SPEI has been extensively described in Vicente-Serrano et al. (2010). Nevertheless, for the sake of completeness, we will describe here the main steps for its computation. Quantifying the SPEI is based on the following steps: (1) calculating the potential evapotranspiration (PET); (2) determining the accumulation of deficit and/or surplus of a climate water balance at different time scales (PET); and (3) normalizing the water balance into a log-logistic probability distribution to obtain the SPEI index series. In order to assess the time evolution of drought conditions in the arid region of northwestern China, the SPEI was calculated according to short (1 and 3 mo), medium (6 and 12 mo), and long (12 and 24 mo) timescales. With a value for PET (according to the Penman equation), the difference between precipitation (P) and PET for month j is calculated according to:

$$D_j = P_j - \mathrm{PET}_j \quad (1)$$

which provides a simple measure of water surplus or deficit for the analyzed month. These calculated D_j values are aggregated at different time series, following the same procedure as that for the SPI. The difference ($D^k_{i,j}$) in a given month (j) and year (i)

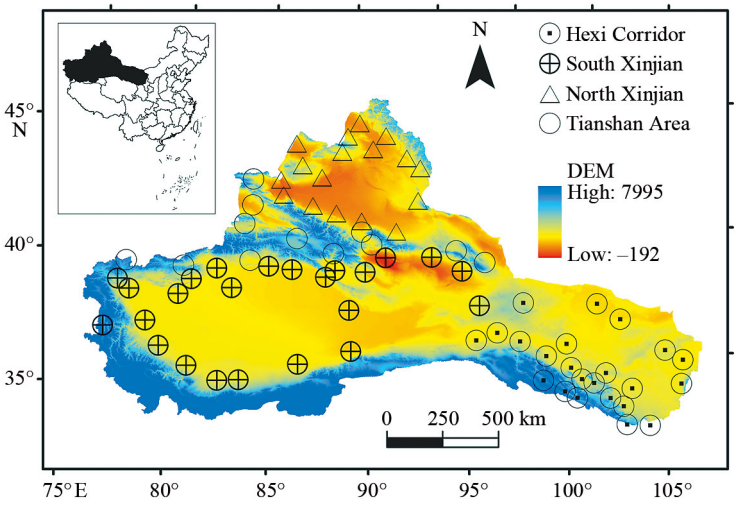

Fig. 1. Study area and weather stations in the arid region of northwestern China

depends on the chosen time scale (k):

$$X_{i,j}^{k} = \sum_{l=13-k+j}^{12} D_{i-1,l} + \sum_{l=1}^{j} D_{i,l} \quad \text{if } j < k, \text{ and} \tag{2}$$

$$X_{i,j}^{k} = \sum_{l=j-k+1}^{j} D_{i,l}, \text{ if } j \geq k$$

where $D_{i,l}$ is the P-PET difference in month l of year i, in mm.

In quantifying the SPEI it is necessary to utilize a 3 parameter distribution, since in 2 parameter distributions, the variable (x) has a lower boundary of zero ($0 > x < \infty$); whereas, in a 3 parameter distribution, the x can take values in the range ($\gamma > x > \infty$), where γ is the parameter of origin of the distribution. Consequently, x can have negative values, which are common in D series. To model the D_i value at different time scales, the probability density function of a 3 log-logistic distribution is used:

$$f(x) = \frac{\beta}{\alpha}\left(\frac{x-\gamma}{\alpha}\right)^{\beta}\left(1+\left(\frac{x-\gamma}{\alpha}\right)^{\beta}\right)^{-2} \tag{3}$$

where α, β, and γ are scale, shape, and origin parameters, respectively, for D values in the range of ($\gamma > D > \infty$). The log-logistic distribution adopted for standardizing the D series for all time scales is given by:

$$F(x) = \left[1+\left(\frac{\alpha}{x-\gamma}\right)^{\beta}\right]^{-1} \tag{4}$$

The $F(x)$ value is then transformed to a normal variable by means of the following approximation:

$$\text{SPEI} = W - \frac{C_0 + C_1 + C_2 W^2}{1 + d_1 + d_2 W^2 + d_3 W^3} \tag{5}$$

where C_0, C_1, C_2, d_1, d_2, and d_3 are constants to SPI; W is a probability-weighted moment, $W = \sqrt{-2\ln(p)}$; and $p \leq 0.5$ is the probability of exceeding a determined D value. The mean value of SPEI is 0, and the standard deviation is 1. The SPEI is a standardized variable, and it can therefore be compared with other SPEI values over time and space. For each time scale, each drought event (the period where SPEI ≤ –1) can be defined according to its duration (the time from beginning to end), severity (the SPEI value for each month following the classification), magnitude (the SPEI sum for each month and for the duration of the severity), and intensity (the magnitude/duration of the event).

In this study, the nonparametric Mann–Kendall method (MK) (Mann 1945, Kendall 1975) was utilized to detect possible trends in drought indices. The results of the MK test were heavily affected by the serial correlation of the time series; thus, we adopted the Yue et al. (2002) method to remove this correlation.

The Pearson correlation was adopted to analyze the relationship between drought time series and climate indices. In order to explore the existence of statistically significant oscillatory components, the wavelet analysis was applied in the time series of the SPEI.

3. RESULTS

3.1. Inter-annual variability of regional SPEI

Fig. 2 shows the evolution of the SPEI over 6, 12, 24, and 48 mo intervals from 1960 to 2010 for the whole study area. We also show the representatives of the SPEI by adding a comparison between the SPEI with the widely used drought index SPI. The evolution of each series of SPEI and SPI was similar (Fig.2), suggesting correlation coefficients between SPI and SPEI in a given time scale are very high, although some differences between them also exist within the study period. The 1987–2005 period clearly exhibited more dry events for SPI than those exhibited using the SPEI. In contrast, the 1960–1986 and 2006–2010 periods qualified as dry using the SPEI; this could mean lower precipitation anomalies were recorded in the arid region of northwestern China (Shi et al.2007).

For the whole study area, the SPEI of short timescales showed a high temporal frequency of dry and moist periods. With increasing timescales, drought

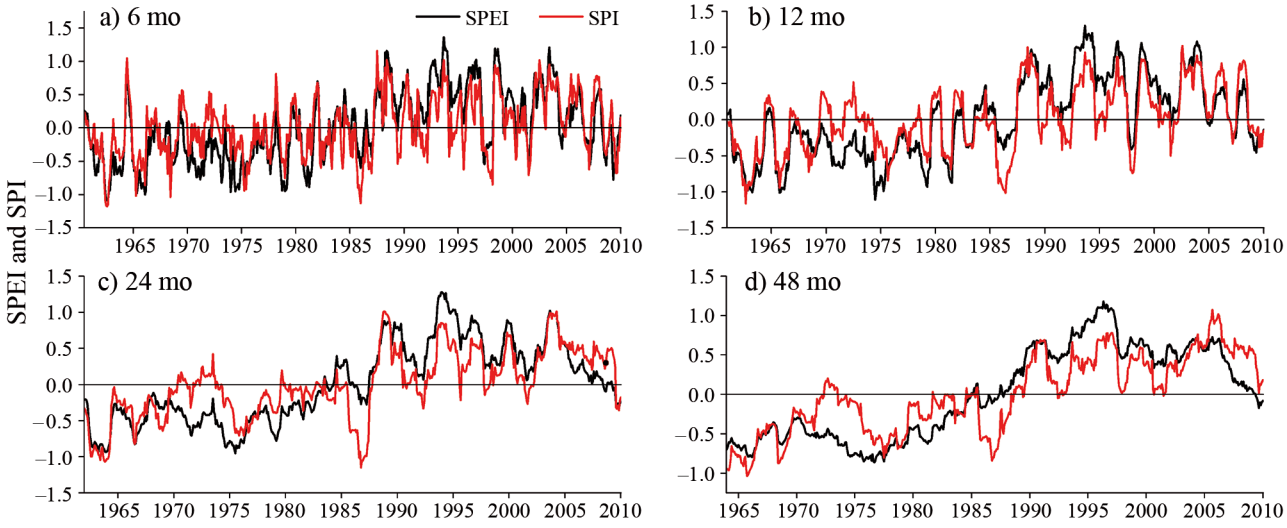

Fig. 2. Drought evolution for the Standardized Precipitation Evapotranspiration Index (SPEI) and Standardized Precipitation Index (SPI) at different time scales ([a] 6, [b] 12, [c] 24, and [d] 48 mo) for the whole study area

and moist periods showed a lower temporal frequency and a longer duration in the study area. Two contrasting periods were evident from 1960 to 2010 for the SPEI. Wet conditions dominated from 1987 to 2010, whereas persistent drought conditions occurred from 1960 to 1987, and were particularly severe from 1973 to 1983. The sub-regions (north Xinjiang, south Xinjiang, and the Tianshan mountains) showed a similar time evolution to the whole study area. For the Hexi Corridor, basic changes of (linear trends) SPEI were the same as the other regions, whereas more fluctuations (positive and negatve SPEI being adjacent to one another) were found in this region .

3.2. Spatial trends of SPEI

Fig. 3 shows the spatial distribution pattern of the temporal trends in SPEI for the 75 meteorological stations, and Fig. 4 presents the regional annual and seasonal anomaly series. For annual SPEI, about 57.3% of the stations have significantly increasing trends. Stations in north and south Xinjiang, especially the stations around the Tarim River Basin, have larger trend magnitudes. Similarly, seasonal SPEI showed increasing trends at ~85 to 90% of the stations (Table 1). The stations presenting larger trend magnitudes were also situated in Xinjiang Province. When examining the regional trends, only the winter SPEI had fluctuations; the annual and other seasonal SPEI showed significant increasing trends (Fig. 4, Table 2).

As seen in Fig. 4, the annual SPEI was negative before 1986, which indicated frequent drought for these times; then, the SPEI became positive, especially from 1990 to 2000. Thus, the SPEI also identified step changes around 1986, and these results were in accordance with climate (temperature and precipitation) change (Shi et al. 2007). We should also note that the SPEI showed falling trends after 2003, which indicated that drought seemed to increase. The evolution of spring, summer, and autumn droughts were the same as the annual drought, whereas fewer droughts were observed before 1975 in these 3 seasons. As in the annual SPEI, seasonal dry (humid) periods also occurred before (after) 1986, although more fluctuation was found in winter.

From the above mentioned results, it is clear that the arid region of northwestern China has locally-significant, positive, wetting trends. Many studies have shown that precipitation has significantly increased over the study area (Zhai et al. 2005, Wang et al. 2013), which is generally consistent with these drought trends. Soil moisture is an important factor for agriculture drought. Wang et al. (2011) showed that the soil moisture in most of Xinjiang had significant upward trends, implying that the SPEI trends were also consistent with moisture trends.

3.3. Frequency estimation with wavelet transform analysis

The wavelet spectrum of wavelet transform was used to analyze the periodic behavior of annual and seasonal SPEI. Fig. 5 presents the periodogram plots of the SPEI patterns in the region and sub-regions. For the whole study area (Fig. 5a), there are 5 clear peaks in the periodogram plot, with 3.9 and 10.8 yr

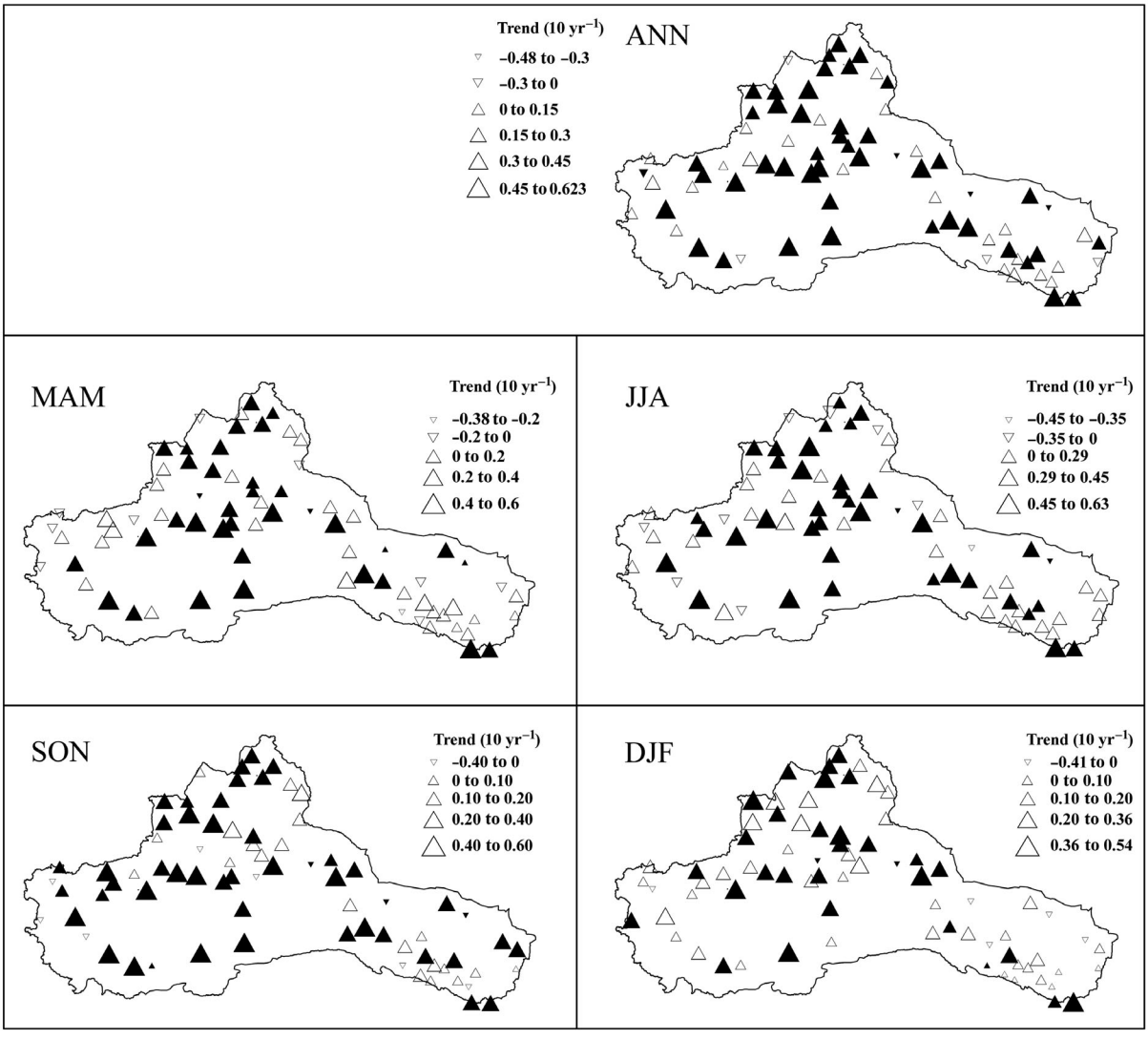

Fig. 3. Spatial decadal trends of SPEI for annual (ANN) and seasonal periods. Black triangles: significant trends at the 0.05 level

being the most significant. North Xinjiang (Fig. 5b) has 3 clear peaks (3.2, 7.7, and 16.2 yr). The cyclical behavior of south Xinjiang suggests that the same pattern as the whole study area is found at small time scales (<5 yr). Additionally, south Xinjiang has a strong 7.7 yr period. This cyclical behavior in the Tianshan mountain area (Fig. 5d) can be observed in the 5.8 and 10.9 yr cycles in the SPEI index. As in the other regions, interannual periods (4.3 yr) and decadal periods (13 yr) are also observed in the Hexi Corridor. Fig. 5 also shows that the periodic characteristics of SPEI at different time scales are similar, denoting that only one time scale of SPEI needs to be applied to characterize the period. Furthermore, the period characteristics become increasingly clear with an increase in time scales.

3.4. Links between regional SPEI and large-scale patterns

The relationship between climate indices and SPEI are shown in Fig. 6. The most significant relationships were observed at 12 and 24 mo scales for both the AO and NAO, with higher correlation coefficients for AO than those of NAO. Southern Xinjiang had closer relationships with AO and NAO, while no significant relationships were observed in the Hexi Corridor. The most significant relationships between MEI and SPEI occurred in south Xinjiang and the Hexi Corridor at the 24 mo scale. For PDO, significant correlations were observed at every region and every scale (except the Tianshan mountains at long times scales), and the most significant relationships

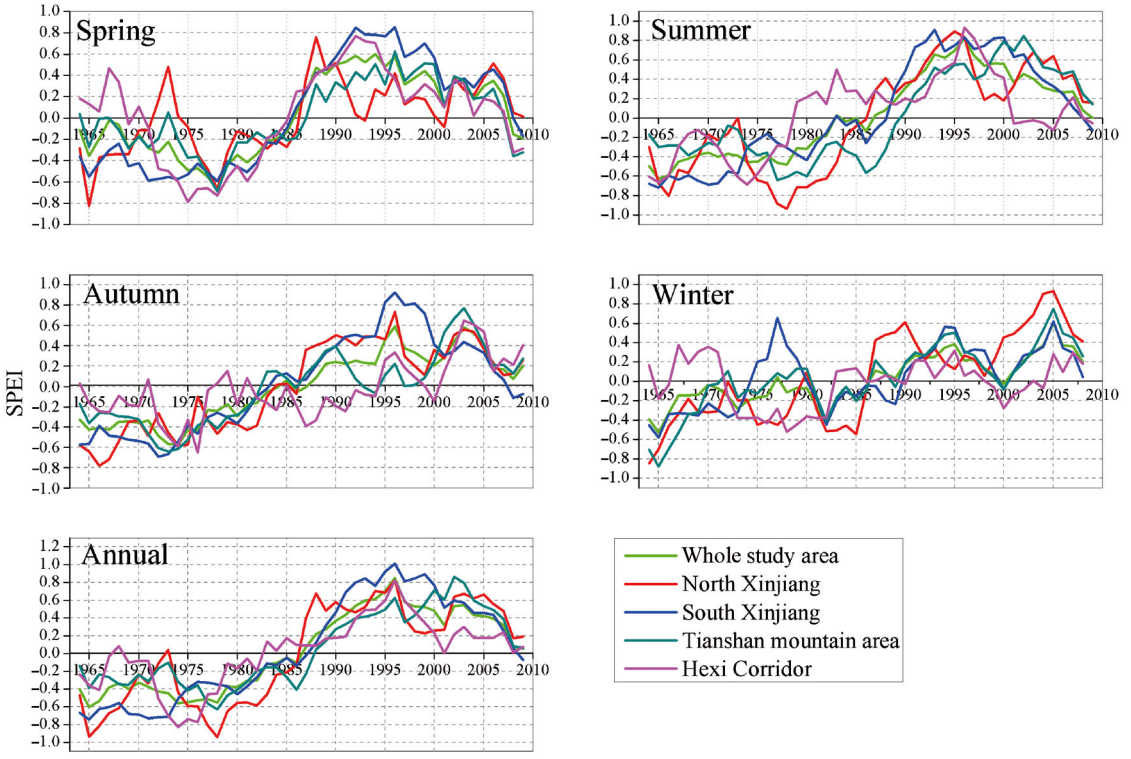

Fig. 4. Regional seasonal and annual time series of the SPEI for 5 yr moving average

were observed in south Xinjiang and the Hexi Corridor. Significant correlations were observed for IOBW in all regions, especially at long time scales. Thus, AO and NAO may only influence the evolution of drought in Xinjiang. Moreover, the PDO and IOBW may affect the whole study area; whereas, with MEI, only south Xinjiang and the Hexi Corridor may be affected.

Table 1. Percentage of stations with significant and insignificant positive and negative trends for annual and seasonal drought from 1960–2010 (in parenthesis are number of stations)

	Significant positive (%)	Insignificant positive (%)	Significant negative (%)	Insignificant negative (%)
Annual	57.3 (43)	32 (24)	5.3 (4)	5.3 (4)
Spring	45.3 (34)	38.7(29)	2.7 (2)	13.3 (10)
Summer	48 (36)	37.3 (28)	2.7 (2)	12 (9)
Autumn	58.7 (44)	28 (21)	4 (3)	9.3 (7)
Winter	38.7 (29)	52 (39)	2.7 (2)	6.7 (5)

Table 2. Regional trends of the Standardized Precipitation Evapotranspiration Index (SPEI). *p = 0.05, **p = 0.01

	All study area	North Xinjiang	South Xinjiang	Tianshan area	Hexi Corridor
Annual	0.227**	0.283**	0.300**	0.198**	0.162*
Spring	0.153*	0.139*	0.233**	0.094	0.094
Summer	0.211**	0.254**	0.260**	0.199**	0.153*
Autumn	0.200**	0.252**	0.239**	0.178**	0.119*
Winter	0.163**	0.251**	0.172*	0.198**	0.037

Correlations between SPEI and climate indices were also analyzed at a monthly scale (Fig. 7). For AO and NAO, strong correlations were observed from January to March, which is the most active period for these 2 atmospheric patterns. Drought was significantly correlated with MEI and PDO from May to August (Fig. 7). For IOBW, more significant relationships were observed for all months, especially at long time scales.

Annual and seasonal relationships between SPEI and climate indices are shown in Fig. 8. The IOBW had significant correlations with SPEI for the entire region and all seasons. The PDO also showed higher correlations with SPEI, especially in spring (MAM) and summer (JJA). The time evolutions of climate indices and SPEI also showed that these 2 time series fit well (not shown), with the exception of some lines.

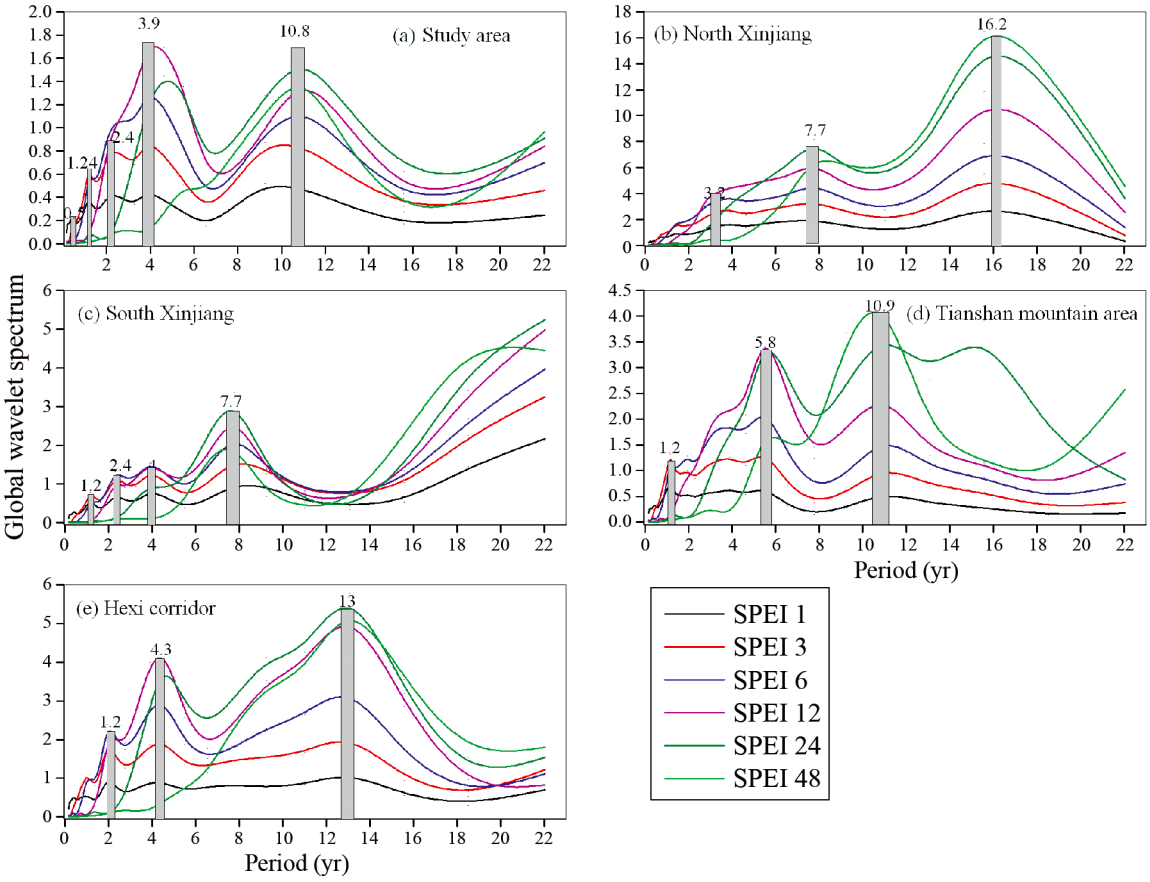

Fig. 5. Global wavelet spectrum of the Standardized Precipitation Evapotranspiration Index (SPEI) at different time scales (1, 3, 6, 12, 24 and 48 mo) for (a) the entire study area, and (b–e) for each region

Drought encompasses a large number of climatological parameters, such as precipitation, temperature, and evapotranspiration. Large scale atmospheric and oceanic circulatory fluctuations have a strong impact on drought evolution. The climatic indices may characterize drought differently through varying considerations of precipitation, temperature, and evapotranspiration. So, some lag times exist between climate indices and SPEI in the arid region of northwestern China. The winter AO and NAO showed significant influences on annual SPEI (the correlation coefficients exceeds 0.4, not shown). Similarly, the summer and spring IOBW and PDO have a statistically significant correlation with annual SPEI in the study area. The seasonal SPEI and climate indices also showed the same lag times. In this study, we only show the relationships between current SPEI and the latest 3 seasonal climate indices (Fig. 9). The spring (MAM) SPEI may be affected by the latest climate indices, especially the IOBW, MEI, and PDO (Fig. 9a,d,g). The winter AO, NAO, and IOBW have significant relationships with the SPEI in the entire arid region. The spring and autumn IOBW had a significant relationship with SPEI in the Xinjiang region; whereas, the spring and autumn MEI only affected south Xinjiang and the Hexi Corridor. For autumn SPEI, droughts in the Xinjiang regions may be affected by winter AO and NAO, and by spring and summer IOBW. Compared with other seasons, relatively low correlation coefficients were observed in winter; however, some significant relationships existed with the former circulation indices only in the Xinjiang regions.

In order to better understand drought characteristics, it is also important to understand teleconnection mechanisms. The Indian Ocean is a part of a large warm water pool (Saji et al. 2006) and the interannual SST variation in the Indian Ocean exerts a substantial influence on the surrounding regions (Tao et al. 2014). The Indian Ocean Basin Mode is the first leading mode of the interannual Indian Ocean SST variability. The tropical Pacific trade winds may have actually strengthened over the past 2 decades, emphasizing the role of Indian Ocean warming relative to Pacific Ocean warming in modulating the Pacific climate changes in the 21st century (Luo et al.

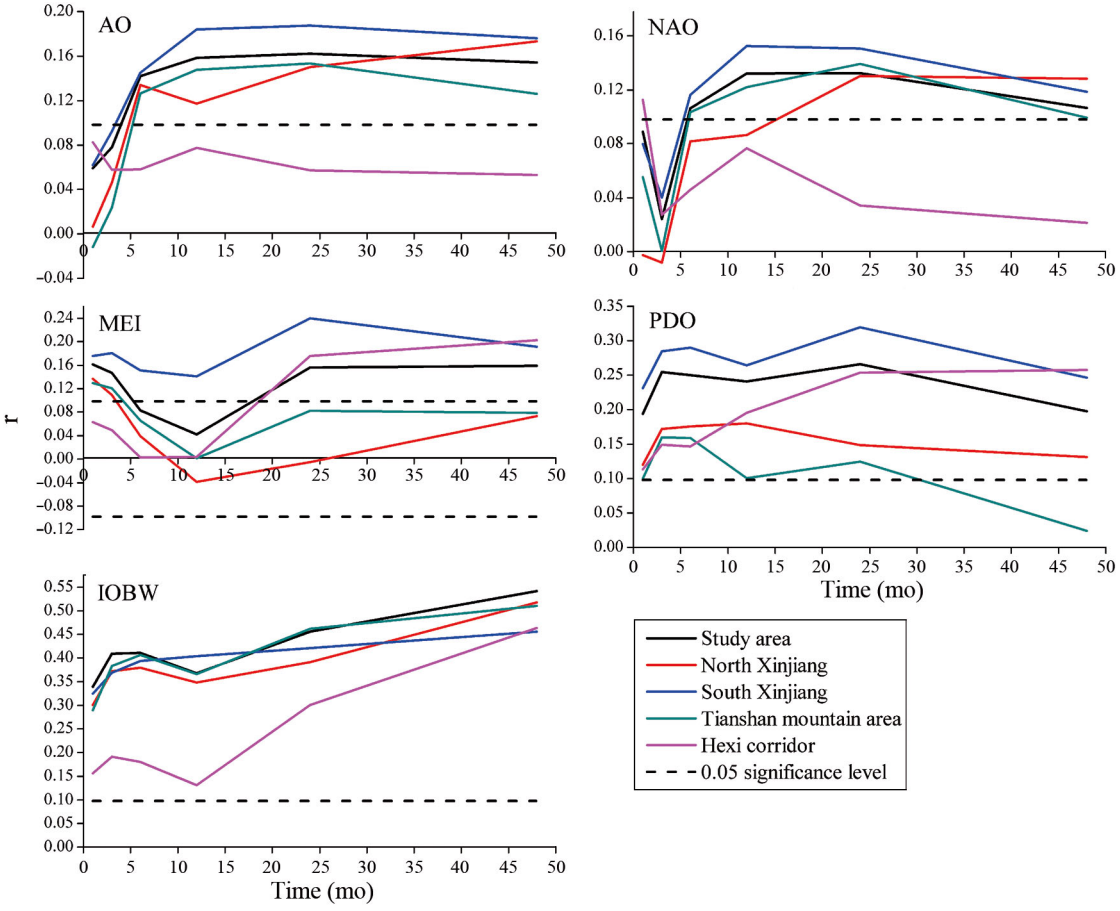

Fig. 6. Regional correlation coefficients between climate indices and the Standardized Precipitation Evapotranspiration Index (SPEI) at various time scales. AO: Arctic Oscillation; NAO: North Atlantic Oscillation; MEI: Multivariate ENSO Index; PDO: Pacific Decadal Oscillation; IOBW: Indian Ocean Basin-Wide mode

2012). Indian Ocean warming leads to precipitation increases over most of the basin, forcing a Matsuno-Gill pattern in the upper troposphere with a strengthened South Asian high (Yang et al. 2007). The water vapor can be transported to the arid region through 2 lines. The eastern line is the vapor through the Bay of Bengal, across the Yarlung Zangbo Grand Canyon and the eastern Qinghai-Tibet Plateau, and then reaching the southeastern arid areas; the West line is vapor through the Arabian Sea, across the Kunlun Mountains and the Pamirs, and then reaching the central and western arid region (Bai et al. 2010). Regarding the PDO, since this is in its warm phase during winter, the Aleutian Low tends to be much lower than normal, while the Mongolian High appears much stronger (but the Siberian High is weaker). As a result, northwestern China is warmer. During summer, the negative SLP anomalies are much weaker in the north Pacific while positive ones are enhanced over eastern Asia, together with a reduced East Asian summer monsoon, a southward-shifted Western Pacific Subtropical High, and a reduced equatorial trade wind. Consequently, northwestern China is wetter (Zhu & Yang 2003). The opposite situation occurs during the PDO cool phase. It is also found that the PDO and the IOBW can modulate the impact of ENSO events on climate variability in China. The drought histories in northwestern China might also indicate a change in the strength of the western and eastern branches of the northward-moving tropical Asian monsoon. On the other hand, it may be that the enhanced activities of ENSO have played an important role in climate changes only in south Xinjiang and the Hexi Corridor.

During the negative phase of the AO, the geopotential height at 500 hPa decreases around Lake Baikal, the Ural blocking high develops, and meridional circulation anomalies prevail over East Asia. Such high-latitude circulation may enhance the cold surge around Lake Baikal and cause it to shift southward, indirectly causing a cold, dry climate in northern China (Shen et al. 2012). During the decade in

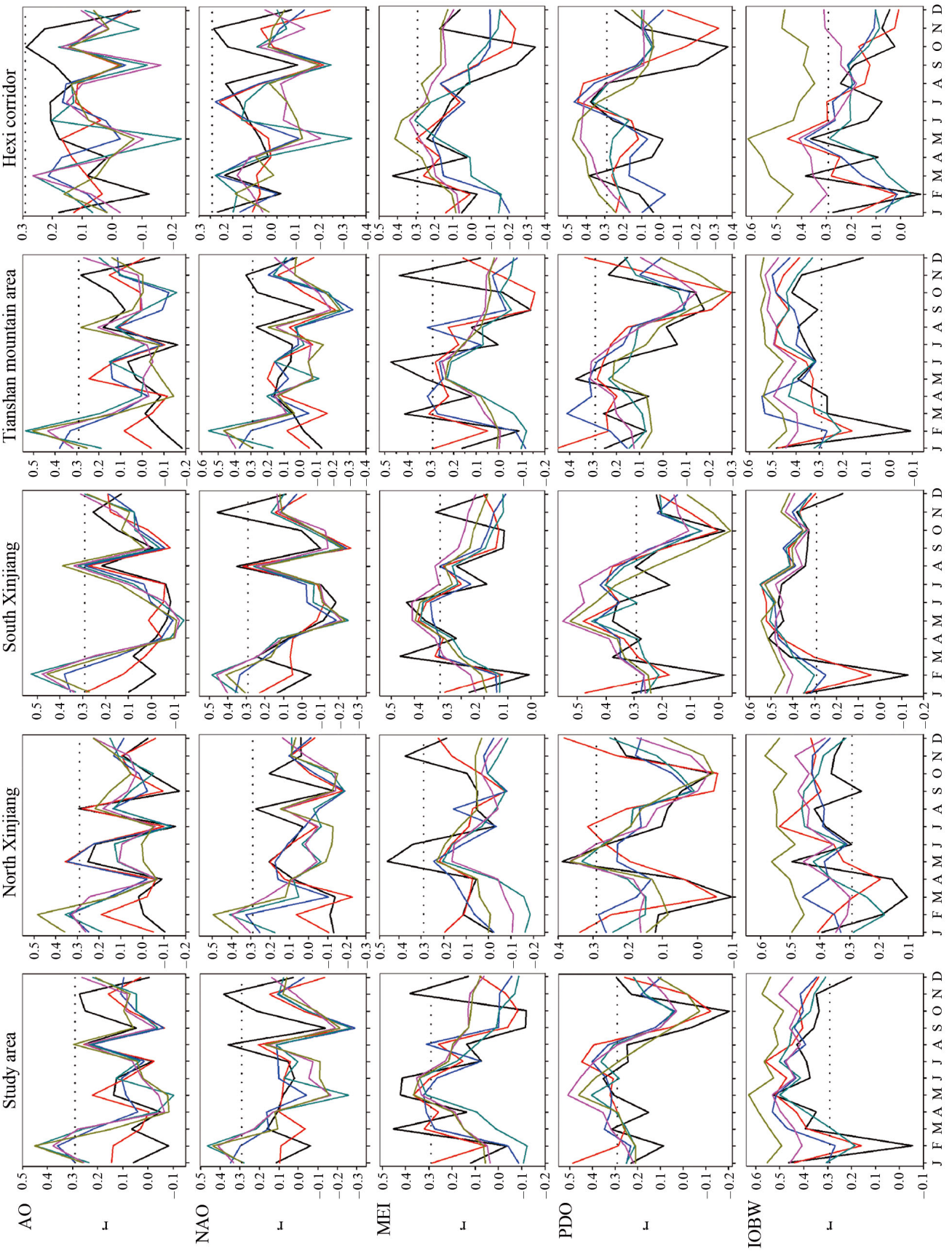

Fig. 7. Monthly correlations between 5 climate indices and regional SPEI at various time scales (1 to 48 mo). See Fig. 6 for acronyms

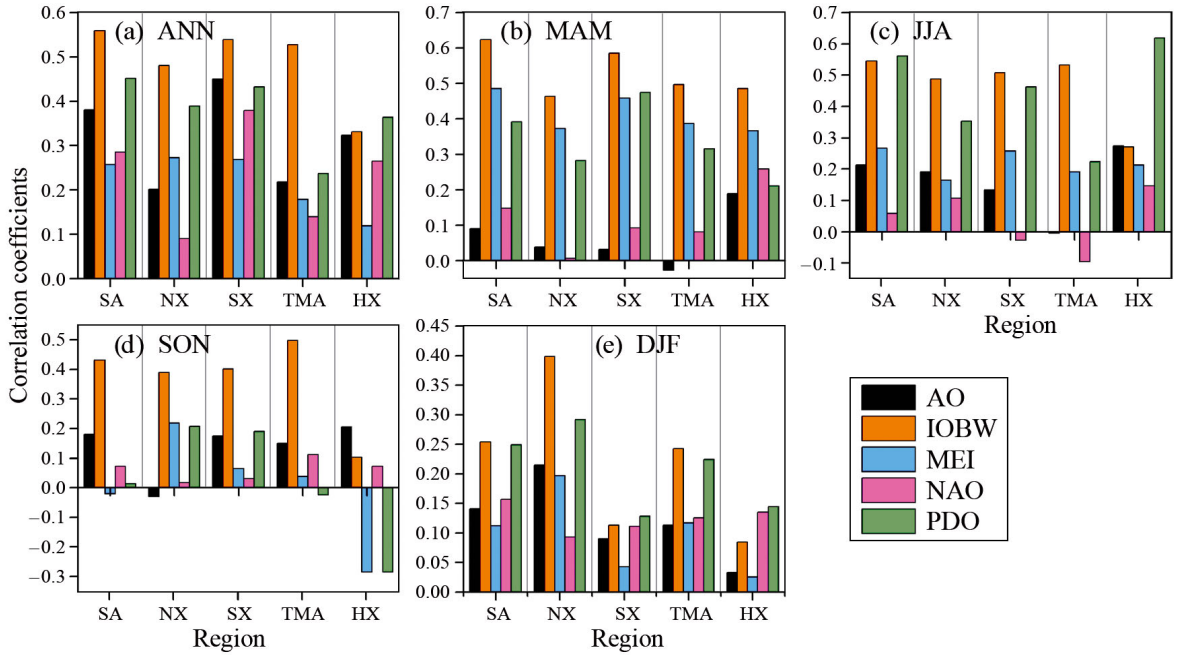

Fig. 8. Correlations of annual (ANN) and seasonal SPEI with respect to climate indices. Correlation coefficient at 1% significance level is ~0.3. SA: whole study area; NX: North Xinjiang; SX: South Xinjiang; TMA: Tianshan mountain area; HX: Hexi corridor; AO: Arctic Oscillation; IOBW: Indian Ocean Basin-Wide mode; MEI: Multivariate ENSO Index; NAO: North Atlantic Oscillation; PDO: Pacific Decadal Oscillation

which the summer AO was stronger than the mean, the East Asian summer monsoon was weaker than normal, such that westerly flows prevailed in the westerly zone of northwest China. This led to more rainfall than the mean, and a wetter climate; whereas, in its monsoon area, the northerly winds are dominant and there is less precipitation than normal, resulting in a climate that is drier than the mean (Wang et al. 2007). NAO is considered as a form of AO in the North Atlantic region (Kerr 1999). Thus, NAO in an extreme negative phase could lead to a precipitation increase in central Asia and northwestern China, owing to an increase in eastward water-vapor transport from southern Europe to northwestern China. Meanwhile, the transient eddy activity becomes intensified in the areas of the north, with a further south route moving from Europe and central Asia throughout northwestern China. In contrast, a dry climate might appear in areas with the occurrence of an extreme positive phase of NAO (Dai et al. 2013).

3.4. Links between spatial SPEI and large-scale patterns

Here we provide a brief overview and potential spatial links between these large-scale patterns. In this section, maps of the Pearson correlation coefficient for the arid region of northwestern China are included at different time scales (3, 12, and 48 mo). These links were evaluated for non-lagged series. The widespread positive correlation pattern between SPEI3 values and the AO index can be seen in southern Xinjiang (Fig. 10). With the increase in time scale, more regions in Xinjiang were observed to have positive coefficients with the AO. The negative and low relationship occurred in the Hexi Corridor and western South Xinjiang. This pattern reveals an obvious link between wet climate and the positive phase of the AO in Xinjiang Province, particularly over southern Xinjiang. The relationship pattern of for the NAO was the same as that for the AO, but with less strength than that for the AO. The MEI index correlation maps present a less homogeneous pattern, with positive values over south Xinjiang. The influence of the MEI pattern on the SPEI is also felt in the middle time scale (i.e. 12 mo) with the largest coefficients. It is immediately noticeable that positive PDO patterns present significant correlations with the SPEI in south Xinjiang, whereas significant negative correlations appeared in the Hexi Corridor and Tianshan mountain area. As expected from the wide basin assessment described in the previous section, the IOBW pattern exerts the largest control, although it gradually loses influence towards eastern

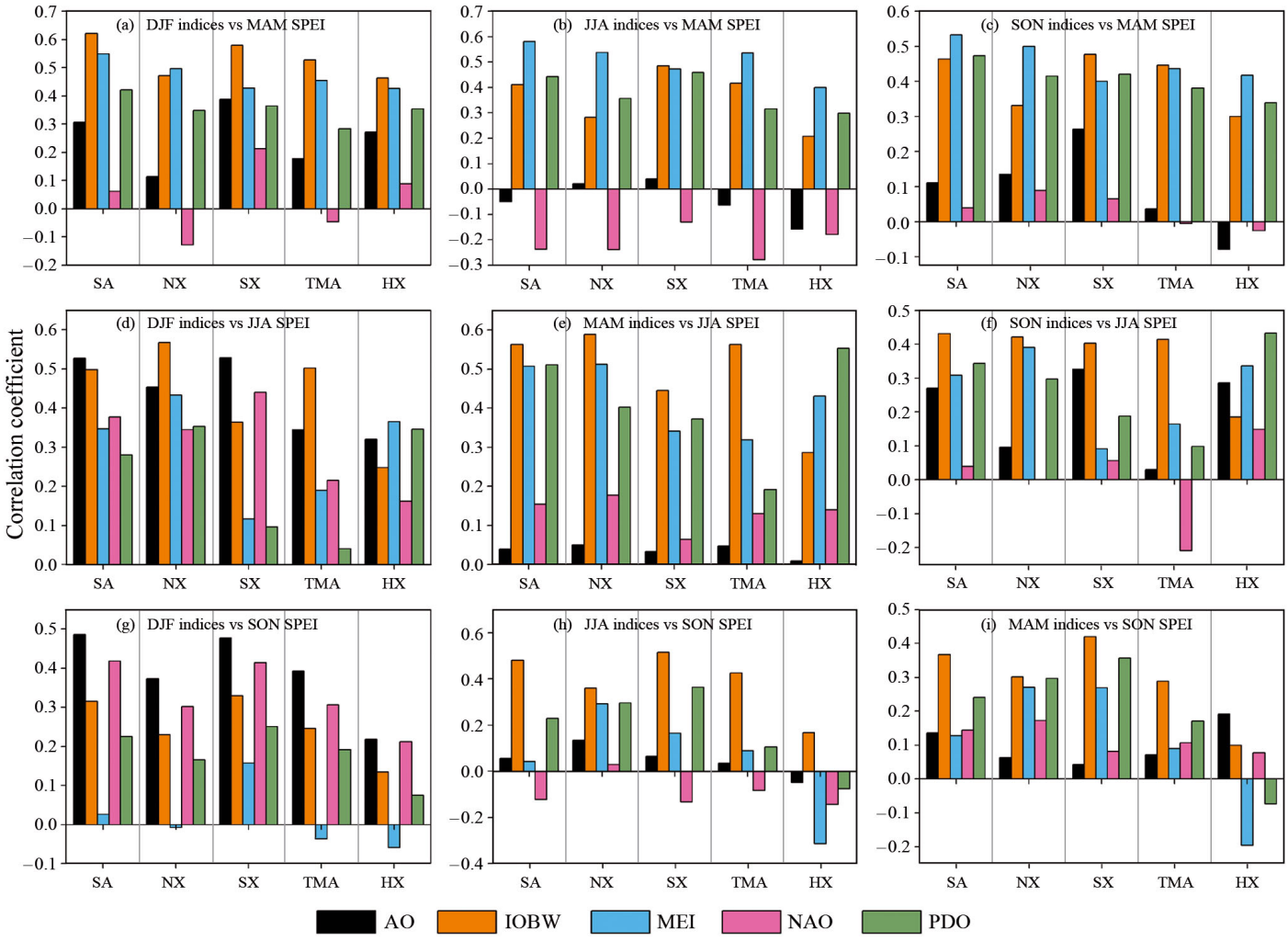

Fig. 9. Correlation coefficients between seasonal SPEI and climate indices with respect to lag times of 3 former seasons. Correlation coefficient at 1% significance level is ~0.3. See Fig. 8 for acronyms

Xinjiang. From the above analysis, we also found that drought in Xinjiang and the Hexi Corridor may be controlled by different atmospheric circulation, due to the inversed correlation patterns for all climate indices.

4. CONCLUSIONS

In this study, we present a multi-scalar drought to assess interannual- and decadal-scale drought and the teleconnections with climate extremes. The results are as follows:

(1) For the arid region of northwestern China, frequent and long droughts occurred from 1960 to 1986; wet climates prevailed from 1987 to 2010. Thus, 1986 is the step change point for drought in the study area. Droughts increased in persistence during the first 26 yr, with greater numbers occurring during the period 1973–1983.

(2) An analysis of annual and seasonal trends of SPEI showed spatial wetting over most regions of the study areas. The stations in Xinjiang Province presented larger trend magnitudes. When examining regional trends, the annual and seasonal SPEI (except for winter) showed significant increasing trends. The annual SPEI was negative before 1986, which indicated frequent drought for this period, and then became positive, especially from 1990 to 2000. We should also note that the SPEI showed decreased trends after 2003, which indicated that drought seemed to increase.

(3) Wavelet analysis was utilized to detect periodical signals of the SPEI in the arid region of northwestern China. Interannual and decadal periods were observed for the whole study area and subregions. The period characteristics at different time scales (1 to 48 mo) were similar, suggesting that only one time scale of SPEI was sufficient to characterize a

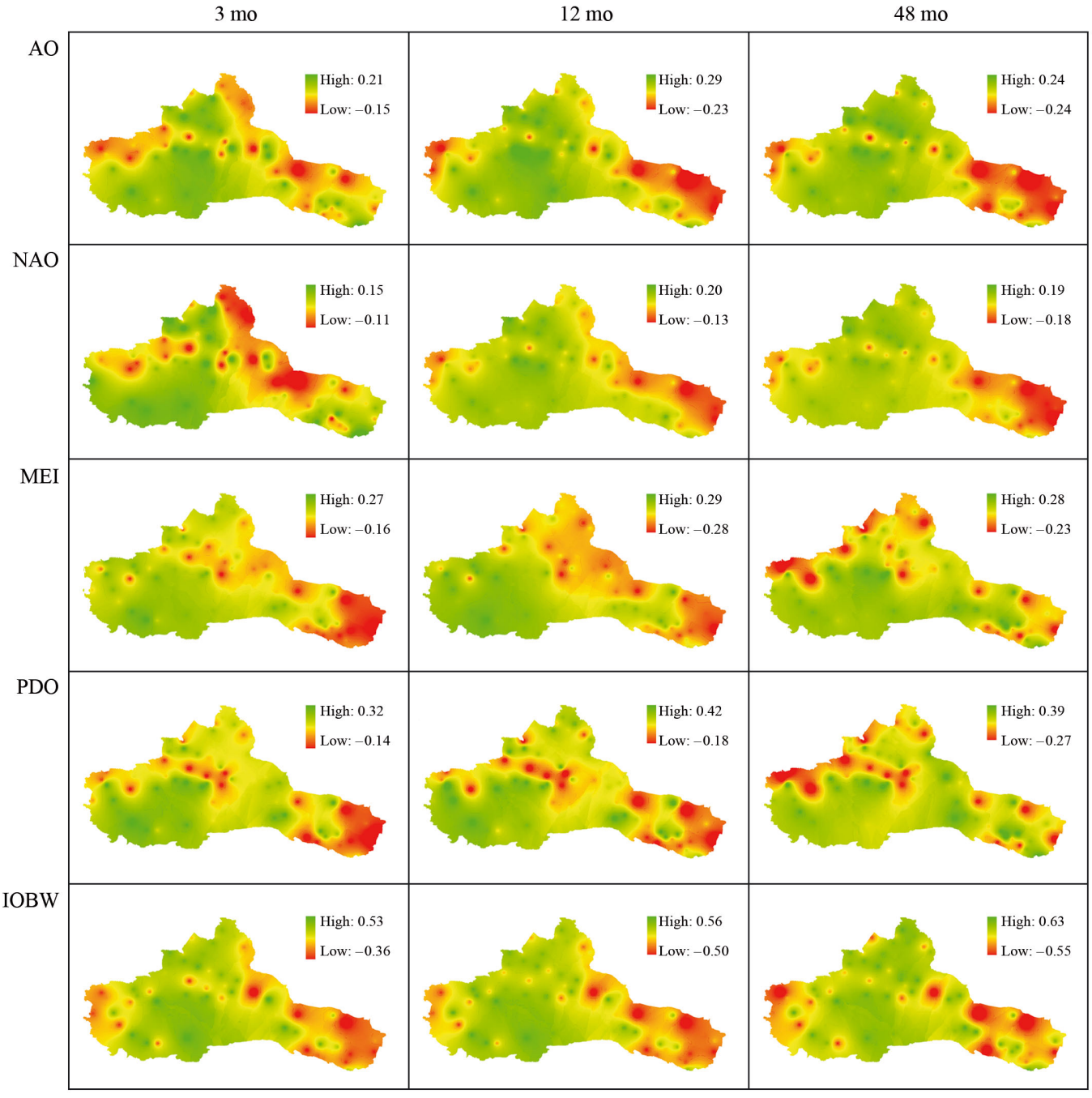

Fig. 10. Spatial correlations between climate indices and Standardized Precipitation Evapotranspiration Index at short (3 mo), middle (12 mo), and long (48 mo) time scales. AO: Arctic Oscillation; NAO: North Atlantic Oscillation; MEI: Multivariate ENSO Index; PDO: Pacific Decadal Oscillation; IOBW: Indian Ocean Basin-Wide mode

particular period. With the increase in time scale, the period characteristics seemed to become increasingly clear.

(4) Significant correlations were observed between IOBW and the whole study area and sub-regions, especially at high time scales, suggesting that the IOBW was the dominant pattern for the study area. Similarly, PDO may also affect the whole study area, whereas AO and NAO may only influence the evolution of drought in Xinjiang. Some lag times may exist between climate indices and SPEI in the arid region of northwestern China, and the current droughts may be affected by the climate indices of former seasons.

There are uncertainties in the SPEI derived from observationally-based station datasets. Although this is arguably the best estimate currently available of continuous and consistent fields of meteorological data, there may nevertheless be unknown biases caused by instrument errors and/or deficiencies in the methodologies. This is especially likely in regions of sparse instrumentation, where, for example, the lack of weather gauges may have a major impact on the accuracy of drought evolution. Likewise, additional research needs to be performed to identify physical mechanisms, rather than only the correlational analysis carried out in this paper.

Acknowledgements. The research is supported by the National Basic Research Program of China (973 Program: 2010CB951003). The authors thank the NCC, CMA, for providing the meteorological data for this study.

LITERATURE CITED

Alexandersson H (1986) A homogeneity test applied to precipitation data. J Climatol 6:661–675

Bai Q, Tian W, Feng Z, Wang C, Jin L (2010) Correlations between the precipitation of Asian arid/semiarid regions and the ocean warm pool climate. J Glaciol Geocryol 32: 295–308 (in Chinese)

Barlow M, Cullen H, Lyon B (2002) Drought in central and southwest Asia: La Niña, the warm pool, and Indian Ocean precipitation. J Clim 15:697–700

Buishand TA (1982) Some methods for testing the homogeneity of rainfall records. J Hydrol (Amst) 58:11–27

Changnon SA, Pielke RA, Changnon D, Sylves RT, Pulwarty R (2000) Human factors explain the increased losses from weather and climate extremes. Bull Am Meteorol Soc 81: 437–442

Dai AG (2011) Characteristics and trends in various forms of the Palmer Drought Severity Index during 1900–2008. J Geophys Res 116:D12115

Dai XG, Wang P, Zhang KJ (2013) A study on precipitation trend and fluctuation mechanism in northwestern China over the past 60 years. Acta Phys Sin 62(12):129201 (in Chinese)

European Communities (2007) Addressing the challenge of water scarcity and droughts in the European Union. Commission of the European Communities, COM (2007) 414 Final, Brussels

Hoerling M, Kumar A (2003) The perfect ocean for drought. Science 299:691–694

Jinsong W, Jiangyong GUO, Yuewu Z, Lanfang Y (2007) Progress and prospect on drought indices research. Arid Land Geogr 30:60–65

Kendall MG (1975) Rank-correlation measures. Charles Griffin, London

Kerr RA (1999) Atmosphere: a new force in high-latitude climate. Science 284:241–242

Li H (2012) The analysis of variation characteristics and cause of drought–wetness over Tarim River basin in the recent 50a. PhD thesis, Nanjing University of Information Science & Technology (NUIST)

Liu C, Chen Y, Xu Z (2010) Eco-hydrology and sustainable development in the arid regions of China preface. Hydrol Processes 24:127–128

Lorenzo-Lacruz J, Vicente-Serrano SM, Lopez-Moreno JI, Begueria S, Garcia-Ruiz JM, Cuadrat JM (2010) The impact of droughts and water management on various hydrological systems in the headwaters of the Tagus River (central Spain). J Hydrol (Amst) 386:13–26

Luo JJ, Sasaki W, Masumoto Y (2012) Indian Ocean warming modulates Pacific climate change. Proc Nat Acad Sci USA 109:18701–18706

Ma ZG, Shao LJ (2006) Relationship between dry/wet variation and the Pacific Decade Oscillation (PDO) in northern China during the last 100 years. Chin J Atmos Sci 30: 464–474

Mann HB (1945) Non-parametric tests against trend. Econometrica 13:245–259

Mishra AK, Singh VP (2010) A review of drought concepts. J Hydrol (Amst) 391:202–216

Mortimore M (2010) Adapting to drought in the Sahel: lessons for climate change. Wiley Interdiscip Rev Clim Chang 1:134–143

Peterson TC, Easterling DR, Karl TR, Groisman P and others (1998) Homogeneity adjustments of *in situ* atmospheric climate data: a review. Int J Climatol 18:1493–1517

Ross T, Lott N (2003) A climatology of 1980–2003 extreme weather and climate events. National Climatic Data Center Tech Rep no. 2003-01. NOAA/NESDIS National Climatic Data Center, Asheville, NC. www.ncdc.noaa.gov/billions/docs/lott-and-ross-2003.pdf.

Saji NH, Xie SP, Yamagata T (2006) Tropical Indian Ocean variability in the IPCC twentieth-century climate simulations. J Clim 19:4397–4417

Santos JF, Pulido-Calvo I, Portela MM (2010) Spatial and temporal variability of droughts in Portugal. Water Resour Res 46:W03503

Shen X, Zhu C, Li M (2012) Possible causes of persistent drought event in North China during the cold season of 2010. Chin J Atmos Sci 36:1123–1134 (in Chinese)

Shi YF, Shen YP, Kang E, Li DL, Ding YJ, Zhang GW, Hu RJ (2007) Recent and future climate change in northwest China. Clim Change 80:379–393

Su M, Wang H (2006) Dry–wet climate variability in China and its relatiosnhips and stability with ENSO. Sci China Ser D 36:951–958 (in Chinese)

Tao H, Borth H, Fraedrich K, Su B, Zhu X (2014) Drought and wetness variability in the Tarim River basin and connection to large-scale atmospheric circulation. Int J Climatol 34:2678–2684

Tao WC, Huang G, Hu KM, Qu X, Wen GH, Gong YF (2014) Different influences of two types of El Niños on the Indian Ocean SST variations. Theor Appl Climatol 117:475–484

Vangelis H, Spiliotis M, Tsakiris G (2011) Drought severity assessment based on bivariate probability analysis. Water Resour Manag 25:357–371

Vicente-Serrano SM, Begueria S, Lopez-Moreno JI (2010) A multiscalar drought index sensitive to global warming: the Standardized Precipitation Evapotranspiration Index. J Clim 23:1696–1718

Vicente-Serrano SM, Begueria S, Lopez-Moreno JI (2011a) Comment on 'characteristics and trends in various forms of the Palmer Drought Severity Index (PDSI) during 1900–2008' by Aiguo Dai. J Geophys Res 116:D19112, doi:10.1029/2011JD016410

Vicente-Serrano SM, Lopez-Moreno JI, Drumond A,

Gimeno L and others (2011b) Effects of warming processes on droughts and water resources in the NW Iberian Peninsula (1930–2006). Clim Res 48:203–212

Vicente-Serrano SM, Lopez-Moreno JI, Lorenzo-Lacruz J, El Kenawy A and others (2011c) The NAO impact on droughts in the Mediterranean Region. In: Vicente-Serrano SM, Trigo RM (eds) Hydrological, socioeconomic and ecological impacts of the North Atlantic Oscillation in the Mediterranean Region, Vol 46. Springer, Dordrecht, p 23–40

Wang JJ, Meng YB (2013) An analysis of the drought in Yunnan, China, from a perspective of society drought severity. Nat Hazards 67:431–458

Wang P, Zheng Y, Sun L, Ren Z, He J, Zhang Q (2007) The inter-decadal correlation between summer Arctic Oscillation and summer drought and moist characteristic of northwest China. Art. No. 66791g. In: Gao W, Ustin SL (eds) Remote sensing and modeling of ecosystems for sustainability IV, SPIE Proc Vol. 6679, San Diego, CA, p 66791G

Wang A, Lettenmaier DP, Sheffield J (2011) Soil moisture drought in China, 1950–2006. J Clim 24:3257–3271

Wang H, Chen Y, Li W, Deng H (2013) Runoff responses to climate change in arid region of northwestern China during 1960–2010. Chin Geogr Sci 23:286–300

Wong G, Lambert MF, Leonard M, Metcalfe AV (2010) Drought analysis using trivariate copulas conditional on climatic states. J Hydrol Eng 15:129–141

Yang D, Shi Y (2002) A preliminary research on relationship between precipitation in spring in Xinjiang and SSTA in the North Atlantic. J Applied Meteorol Sci 13:478–484 (in Chinese)

Yang JL, Liu QY, Xie SP, Liu ZY, Wu LX (2007) Impact of the Indian Ocean SST basin mode on the Asian summer monsoon. Geophys Res Lett 34:L02708, doi:10.1029/GL028571

Yu M, Li Q, Hayes MJ, Svoboda MD, Heim RR (2014) Are droughts becoming more frequent or severe in China based on the Standardized Precipitation Evapotranspiration Index: 1951–2010? Int J Climatol 34:545–558

Yue S, Pilon P, Phinney B, Cavadias G (2002) The influence of autocorrelation on the ability to detect trend in hydrological series. Hydrol Processes 16:1807–1829

Zeng N (2003) Drought in the Sahel. Science 302:999–1000

Zhai PM, Zhang XB, Wan H, Pan XH (2005) Trends in total precipitation and frequency of daily precipitation extremes over China. J Clim 18:1096–1108

Zhang S, Fang B (1995) China disaster report. China Statistics Press, Beijing 52:112 (in Chinese)

Zhu Y, Yang X (2003) Relationships between Pacific Decadal Oscillation (PDO) and climate variabilities in China. Acta Meteorol Sin 61:641–654

Editorial responsibility: Tim Sparks, Cambridge, UK

Submitted: March 26, 2014; Accepted: October 7, 2014
Proofs received from author(s): November 28, 2014